ESRF	**Experiment title:** **Microscopic origin of magnetostriction in FeCoB amorphous alloys studied by Differential EXAFS**	**Experiment number**: HD-257
Beamline:	**Date of experiment**: from: 25 June 2008 to: 1 July 2008	**Date of report**: 12 August 2008
Shifts:	**Local contact(s)**: Sakura Pascarelli	*Received at ESRF:*

Names and affiliations of applicants (* indicates experimentalists):

*Javier Diaz**,** *Carlos Quiros, *Luis Manuel Alvarez del Prado

Universidad de Oviedo

REPORT:

Differential EXAFS has been used to identify the atomic environments involved in the magnetostriction effect. This technique was able to distinguish only those Fe and Co atomic environments that changed their bond length when a magnetic field was applied. The study was done in amorphous and polycrystalline FeCoB films, 6 μm thick, with different compositions and, therefore, different magnetostriction coefficients. Two films were deposited with the same relative transition metal (TM) concentration ($Fe_{80}Co_{20}$), but changing their boron atomic concentration from below (10%) to above (20%) the eutectic concentration (17%)of the binary TM-boron alloy. This relatively small change in boron content was used to modify the microstructure of the film, from polycrystalline (10% at. boron) to amorphous (20% at. boron). For the other two analyzed films, boron concentration was 20%, i.e., the films were amorphous, but their relative concentrations of Fe and Co were changed to have alloys with majority Fe ($(Fe_{80}Co_{20})_{80}B_{20}$), majority Co ($(Fe_{10}Co_{90})_{80}B_{20}$) or equivalent concentrations of Fe and Co ($(Fe_{50}Co_{50})_{80}B_{20}$). The magnetostriction coefficients decreased with Co content, being of about 31 ppm in $(Fe_{80}Co_{20})_{80}B_{20}$ and lower than 0 in $(Fe_{10}Co_{90})_{80}B_{20}$ [1].

The most important conclusions of the analysis were:

(1) Only some Fe and Co environments were magnetostrictive. They differed notably from the non magnetostrictive environments in bond length and atom arrangement. The analysis showed that, in fact, the EXAFS spectra were better fitted and the extracted parameters were more coherent using a two phase model.

(2) The crystal structure of the polycrystalline film was bcc.

(3) The rest of the films with higher boron concentration were in the amorphous phase, manifested by lower EXAFS amplitudes and less intensity from second neighbor shells. However, this amorphous phase retained some short range order which fitted well to an fcc crystal structure. The fit of the spectra distinguished up to the third shell. The Fe-TM and Co-TM bond lengths of the non-magnetostrictive phase were, at least, 0.1 A smaller than in the pure crystal form.

(4) The analysis discarded magnetostrictive Fe-Co environments. Fe and Co magnetostrictive phases were somehow activated by boron since their concentration increased with their relative boron content.
(5) The magnetostrictive environments had longer bond lengths than the average bond length in the alloy. The magnetostriction coefficients were positive for Fe in any of the films.
(6) Co magnetostrictive environments were detected by DiffEXAFS in the Co rich film only. They were also detected indirectly in the EXAFS spectrum of the film with the lowest Co composition. Its magnetostriction coefficient was negative.

The effect of Boron concentration

The atomic Boron concentration at the eutectic point in the TM-B phase diagram is 17% boron. At this concentration, the TM-B alloy becomes amorphous. The transition from the polycrystalline to the amorphous phase is rather sharp: a large proportion of the alloy was in a polycrystalline state when boron concentration was 10% at. The alloy became amorphous when boron atomic concentration was 20%. The EXAFS spectra of $(Fe_{80}Co_{20})_{90}B_{10}$ and $(Fe_{80}Co_{20})_{80}B_{20}$ shown in figure1 demonstrated this dependence of the atomic structure of the the alloy with boron concentration. The analysis of the low boron concentration EXAFS spectra using a single phase model showed that Fe and Co were in a bcc structure, and that Fe seemed to have sensibly longer bond lengths than Co. In the 20% B concentration film, the amplitude of the EXAFS signal was significantly reduced and second neighbors intensity was much smaller, typical of atomically disordered structures. Even though, some short range order was retained. The spectra analysis showed an fcc arrangement in either Fe and Co. Also, bond lengths in Fe resulted to be significantly longer than in Co: the first shell in Fe was at 2.45 A, whereas in Co it was found at 2.34 A.

Both films had magnetostrictive environments in Fe, but none were detected in Co by DiffEXAFS (figures 2). In the polycrystalline film, the structure of the magnetostrictive environments was also bcc, as in the EXAFS spectra, but bond lengths were longer, about 0.1 A in the first shell (figure 3). Disorder was stronger in the magnetostrictive environments, in view of the large Debye-Waller factors obtained: 0.018 A^2 against 0.006 A^2 in the non-magnetostrive phase. In the amorphous sample, (20% at. B), the bond length of the Fe atoms was 2.63 A, substantially longer than the obtained in the EXAFS spectra, 2.45 A (figure 4). Although the magnetostrictive environment showed some intensity at second neighbors, this was too weak and the spectra too noisy to be identified. Nevertheless, it was more related to a bcc structure than to the fcc found in the EXAFS spectra, as it can be seen when both spectra were compared (figure 4).

The different atomic environments found in DiffEXAFS and EXAFS indicates that the samples were a mixture of, at least, two phases, one *magnetostrictive*, detected by DiffEXAFS, and *no-magnetostrictive* the other. Differential EXAFS does not give the atomic coordination as in EXAFS, because the amplitude of the differential spectra is proportional to the magnetostrictive strain, i.e., to the magnetostrictive coefficient of that particular environment, which is, a priori, unknown. The relative proportion of each of the phases was obtained then from the EXAFS spectra which contained both phases. To do this, the parameters obtained from the analysis of the DiffEXAFS spectra, shell size and Debye –Waller factor, were used to simulate its EXAFS spectrum. This was included in the simulation of the EXAFS spectrum of the alloy together with the other scattering paths used previously for the fit. Then, the resulted amplitude of the simulated EXAFS spectrum yielded directly the concentration of the magnetostrictive and non-magnetostrictive phase in the alloy. This amplitude was also the one used to determine its magnetostriction coefficient. The way of how the magnetostriction coefficients of the magnetostrictive phase and the alloy were extracted from the data will be explained later.

The concentration of Fe atoms in the magnetostrictive phase in the polycrystalline alloy was of about 65(5)% of the total concentration of Fe atoms in the alloy (Figure 5). The remaining non-

magnetostrictive phase had similar bond lengths and Debye-Waller factors than in the spectrum of Co, indicating that Fe and Co should be mixed. However, this mixture did not generate magnetostrictive environments since no signal was appreciated in the DiffEXAFS spectrum of Co, and the magnetostrictive environments found in Fe had sensibly different bond lengths than Co.
The amorphous $(Fe_{80}Co_{20})_{80}B_{20}$ alloy contained 46(5)% of its Fe atoms in the magnetostrictive phase (figure 6). The Fe bond length in the remaining non-magnetostrictive phase was 2.43 A in the first shell, smaller than in the FeCo crystalline phase (2.48 A), and still too big compared to the obtained in Co (2.36 A), suggesting that Fe and Co were largely segregated from each other in this alloy.

The effect of increasing Co concentration in the amorphous FeCo alloys

When Fe and Co concentration were the same, DiffEXAFS was again only visible in the Fe environments. The spectrum was similar to the measured in the amorphous alloy with 64% Fe but more noisy and with smaller amplitude due to the lower amount of Fe in the alloy (figure 7). This made difficult its analysis. Then, it was assumed that the magnetostrictive environments were the same than the measured in the amorphous alloy with higher Fe content. Its concentration in the film was estimated by EXAFS using the method explained before. The analysis showed that the proportion of magnetostrictive Fe atoms in this film actually increased: they were about 60% of the alloy (figure 8). This was an increment of about 10% with respect to the found in the film with a higher Fe concentration. The bond length of the non-magnetostrictive Fe phase was similar than in that film. However, Co bond length increased to 2.41 A, approaching that of non magnetostrictive Fe (2.43 A).
When Co was majority (90%), no magnetostrictive signal was detected in Fe, probably because its concentration was too low and fell below the detection limit of DiffEXAFS. However, Co presented magnetostrictive environments (figure 9). Differently to Fe, this environment was composed of two distinct atomic sites, one at about 2.49 A, and the other at 2.76 A, and its strain was negative, i.e., their bond length shrunk in the presence of a magnetic field (figures 9 and 10). EXAFS analysis showed that its concentration was of about 40%.The non magnetostrictive Co phase (fgure 11) had a bond length of 2.45 A.
In view of the observed Co magnetostrictive environments in the sample with 72% at. Co, it is likely that these environments were not identified by DiffEXAFS in the alloys with lower Co concentration because their signal was below the detection limit of the technique. An indirect way to detect these magnetostrictive environments in these alloys was to use the same method utilized to estimate the concentration of the magnetostrictive environments in Fe, i.e., include its simulated EXAFS spectrum in the fit of the EXAFS spectrum of the alloy. This estimation assumed that the magnetostrictive environment, bond lengths and Debye-Waller factors, did not change with the relative concentrations in the alloy, as it seemed to happen in the case of Fe. The presence of a Co magnetostrictive phase was only investigated in the film with the lowest Co content. Unfortunately, no EXAFS spectra was available (in transmission) of the $(Fe_{50}Co_{50})_{80}B_{20}$ film. Figure12 shows the EXAFS spectrum (χ(R)) of $(Co_{90}Fe_{10})_{80}B_{20}$ at the Co K edge compared with the spectrum of the same film at the Fe edge, and with the EXAFS spectrum of the Co rich alloy at the Co K edge. It is clearly different than the two spectra. Its main peak was downshifted, indicating shorter bond lengths, and second neighbor shape and intensity did not match that of the other two spectra. It is, however, more similar to the χ(R) of the Co magnetostrictive environment observed by DiffEXAFS in $(Co_{90}Fe_{10})_{80}B_{20}$ (figure 9). The EXAFS analysis estimated that the concentration of magnetostrictive Co in $(Fe_{80}Co_{20})_{80}B_{20}$ was of about 60% of the total amount of Co atoms. The non-magnetostrictive phase had Co bond lengths (2.4 A) that approached those of non-magnetostrictive Fe (2.43 A) in the same alloy. On the other hand, the same analysis done in the EXAFS spectrum of the polycrystalline alloy at the Co K edge did not register the presence of any magnetostrictive environment similar to the found in the Co rich sample or in the Fe environments of the same polycrystalline film.

Calculation of the Magnetostriction coefficients

This experiment showed that only a certain proportion of atoms participated in the magnetostriction effect. Therefore, the macroscopic magnetostrictive coefficients were estimated taking into account the concentration and magnetostrictive coefficient of each of the magnetostrictive environments detected by DiffEXAFS. The magnetostriction coefficient of the magnetostrictive phase, λ_m, was obtained in the following way: $\lambda_m=\delta R/R$, where δR was the displacement between atoms due to the magnetic field, and R was the distance between those atoms. The amplitude of the DiffEXAFS spectra was proportional to δR: $A_d=2A_e\delta R$, where A_e was the amplitude of the magnetostrictive environment extracted from the EXAFS spectrum of the alloy. Note that A_e was obtained from the non-normalized EXAFS spectrum. R was deduced from the fitting of the DiffEXAFS spectrum. Then, $\lambda_m= A_d/2A_eR$.

The macroscopic magnetostriction coefficient λ_M was estimated from the magnetostriction coefficient of the magnetostrictive environments detected by EXAFS as follows: $\lambda_M=\delta L/L$, where δL was the length change of the material in the magnetic field direction, and L was the material's initial length with no magnetic field applied. δL was caused by the different magnetostrictive environments present in the material. L included the length of the magnetostrictive and non-magnetostrictive phases: $L=L_m+L_{nm}$. It was assumed that the length of each phase was isotropic in average, i.e., it was the same in any direction of the film. Since $\lambda_m=\delta L/L_m$, $\lambda_M= \lambda_m/(1+L_{nm}/L_m)$. L=NR, where N was the number of atoms in the measuring direction and R was their bond length. Then, $\lambda_M= \lambda_m/(1+\alpha R_{nm}/R_m)$, where α was the ratio between the total number of atoms of each of the phases in the total length L, which was equivalent to the ratio between their atomic concentrations in the alloy , which was the ratio of their corresponding coordination numbers obtained from EXAFS. Note that the non-magnetostrictive environments included those of Co and Fe. Because the short B-TM bond length, it was assumed that B occupy interstitial sites. This means that the term $(1+\alpha R_{nm}/R_m)$ was better written as follows:

$$(1+\alpha R_{nm}/R_m)=(N_mR_m+N_{nm}R_{nm})/N_{nm}R_{nm}$$

and

$$N_{nm}R_{nm}= (N_{nm}R_{nm})_{Fe}+(N_{nm}R_{nm})_{Co}$$

For example, in the case of $(Fe_{80}Co_{20})_{80}B_{10}$:

$$(N_mR_m+N_{nm}R_{nm})/N_{nm}R_{nm}=\{(N_mR_m)_{Fe}+[(N_{nm}R_{nm})_{Fe}+(N_{nm}R_{nm})_{Co}]\}/ (N_mR_m)_{Fe}$$

$$(N_mR_m+N_{nm}R_{nm})/N_{nm}R_{nm}=\{0.8*0.65*8*2.59+[0.8*0.35*8*2.48+0.2*8*2.48]/(0.8*0.65*8*2.59)$$

$$(N_mR_m+N_{nm}R_{nm})/N_{nm}R_{nm}=1.884$$

Magnetostriction coefficients

$(Fe_{80}Co_{20})_{80}B_{10}$: its magnetostriction phase was a bcc crystal. Therefore, it had two magnetostriction coefficients related to the 100 and 111 directions of the crystal. DiffEXAFS measures the interatomic distance difference between applying the magnetic field in a given direction and its perpendicular. The linear polarization of the incident beam selects the direction of measure. It was either parallel or perpendicular to the magnetic field. In a polycrystal with the crystallites randomly oriented, only those crystals with their crystallographic directions oriented parallel to the polarization vector contributed the most to the EXAFS and DiffEXAFS spectrum. Therefore, the DiffEXAFS experiment was similar to measure the magnetostriction of a monocrystal in each of the crystallographic directions by the method of measuring the difference in strain between applying the magnetic field parallel to the chosen crystallographic direction and perpendicular to it. The important difference is that, in a polycrystal, DiffEXAFS measures the strain in all the crystallographic directions all at once. In this sample, the structure was bcc. The expression for the strain in a cubic crystal for a given measure and magnetization directions is well known. When this expression is applied to calculate δR along the (100) and (111) directions in the present experiment, i.e., δR as the difference in strain applying the magnetic field parallel or perpendicular to the crystal direction ($\delta R = \delta R(0º)- \delta R(90º)$), $\delta R =(3/2)\lambda_{111}$ and $\delta R =(3/2)\lambda_{100}$. Bearing this (3/2) factor in mind, the resulted magnetostriction coefficients were:

λ_{111}=29 ppm and λ_{100}=42 ppm.

Assuming that the crystallites in the alloy did not have any preferential orientation in the plane,

$\lambda_m=(2\lambda_{100}+3\lambda_{111})/5=34.4$ ppm

Then,

$\lambda_M= \lambda_m/[(N_mR_m+N_{nm}R_{nm})/N_{nm}R_{nm}]$

λ_M=34.4/1.884=18.26 ppm

$(Fe_{80}Co_{20})_{80}B_{20}$: the magnetostriction coefficient of the magnetostrictive phase was:

λ_m=51 ppm

The macroscopic magnetostriction coefficient, assuming that Co had no magnetostrictive environments, was:

λ_M=51/[0.8*0.46*2.63+(0.2*2.36+0.8*0.54*2.43)]/(0.8*0.46*2.63)

λ_M=51/2.57=19.8 ppm

$(Fe_{50}Co_{50})_{80}B_{20}$: the magnetostriction coefficient of the magnetostrictive phase derived from the parameters obtained from the EXAFS spectrum of this alloy:

λ_m=63 ppm

This is about 20% higher than in the alloy with 64% at. Fe. It should be similar because the magnetostrictive environment was the same in both samples. This is indicative of the error bars involved in the determination of the magnetostrictive coefficients in this experiment, something that will be discussed later on.

The macroscopic magnetostriction coefficient, assuming again that Co had no magnetostrictive environments, was:

λ_M=63/[0.5*0.6*2.63+(0.5*2.4+0.5*0.4*2.43)]/(0.5*0. 6*2.63)

λ_M=63/3.14=20.1 ppm

$(Fe_{10}Co_{90})_{80}B_{20}$: Here, only Co magnetostriction was measured since Fe EXAFS signal was too weak. The magnetostrictive phase had two components, one at R_1=2.3 A and the other at R_2=2.76 A. Their corresponding magnetostrictive coefficients were λ_1=-91 ppm and λ_2=-75 ppm. Averaging over the two components:

λ_m=-83 ppm

This value is of the same order than the observed in hcp Co crystal for certain crystal directions respect to the *c* axis.

The macroscopic magnetostrictive coefficient that should be measured in this alloy is:

λ_M=-83/[0.4*0.9*2.3+(0.1*2.45+0.9*0.6*2.45)]/(0.4*0. 9*2.3)

λ_M=-83/2.9=-28.7 ppm

This value is about 10 times much higher than the expected. It might happen that the remaining Fe compensated this negative magnetostriction. If all Fe was in the magnetostrictive amorphous phase observed by DiffEXAFS in the other amorphous samples, the macroscopic magnetostriction would be:

$\lambda_M=(L_{mCo}\lambda_{mCo}+L_{mFe}\lambda_{mFe})/(L_{mCo}+L_{mFe}+L_{nm})$

$\lambda_M =(N_{mCo}R_{mCo}\lambda_{mCo}+ N_{mFe}R_{mFe}\lambda_{mFe})/(N_{mCo}R_{mCo} +N_{mCo}R_{mCo} + N_{nm}R_{nm})$

In this case,

λ_M =[0.4*0.9*2.3*(-83)+ 0.1*2.63*(63)]/[0.4*0.9*2.3+0.1*2.63+ 0.9*0.6*2.45]

λ_M=(-68.724+16.569)/2.414=-21.6 ppm

which is still much higher than the expected.

The macroscopic magnetostrictive values are close to the values expected in these alloys if the magnetostrictive component of Co was not taken into account. On the other hand, the sign of the Co magnetostrictive phase seems to be correct and its magnetostrictive coefficient is not too far from the observed in hcp Co.

Discussion

From these measurements, it seems clear that boron must be behind the magnetostrictive properties of the alloys. DiffEXAFS data discard significant magnetostrictive contributions

from Fe-Co environments. Moreover, EXAFS data showed that the mixing of Co and Fe was poor in the amorphous alloys since their bond lengths did not match and disorder, evidenced by their Debye-Waller factor and coordination numbers, was stronger in Fe. This has been already observed in similar kind of alloys also by EXAFS [6]. If EXAFS spectra were fit assuming that only one phase was present, the difference between Co bond length and Fe bond length increased with the relative concentration of boron (figure 14). Moreover, when the relative concentration of boron respect to the TM increased, the bond length of Fe increased, but it decreased in Co. This in agreement with the increased concentration of the magnetostrictive phase as the relative boron concentration increased. When the magnetostrictive phase was introduced in the fits, Co and Fe bond lengths approached each other but only in the case of the polycrystalline sample Co environments were similar to those of Fe. The approach in bond length was also significant in the Co rich sample, but that should not mean that their environments were the same. In this sample, Co had the lowest concentration of boron and Fe the highest. The lower concentration of boron impurities in Co might have "enlarged" their bond lengths respect to the other films (the first neighbor distance in fcc Co is 2.51 A). On the other hand, the higher relative concentration of boron in Fe decreased its bond length in the non-magnetostrictive phase and increased the bond length in the magnetostrictive phase. Fe bond length was larger in $(Fe_{50}Co_{50})_{80}B_{20}$ which had a lower boron concentration relative to Fe, suggesting that its magnetostriction phase concentration was the highest. The data showed in figure 14 come from EXAFS spectra taken in 100 nm thick samples in fluorescence detection, i.e., the samples were not the same as the analyzed by transmission although, nominally, they had the same composition.

The exact relative proportion of boron bonded to either Fe or Co in the analyzed films is rather complex to calculate. It should depend on the relative Fe and Co concentrations and on the boron diffusivity and chemical affinity for each of the transition metal species. It seems that boron bonds preferentially to Fe [6]. The analysis of the EXAFS spectra showed more disorder in Fe than in Co in all the studied alloys, which was an indication of that trend. But it is clear that, for the same boron concentration, the quantity of boron bonded to either Fe or Co was bigger when their concentration in the film was smaller. Then, the increase in the concentration of the Fe magnetostrictive phase in Fe from 46% to 60% when the alloy decreased its atomic Fe concentration from 64% to 40% could be explained noting that the relative atomic concentration of boron to iron increased from 24% to 33%. In the case of the Co magnetostrictive environments, its concentration increased from 40% to 60% in Co when the relative atomic concentration of boron changed from 22% to 50%.

Atom arrangement was also different in the amorphous state (fcc) than in the polycrystalline (bcc). EXAFS analysis showed that the amorphous phase retained an fcc short range order that extended up to third neighbors. Fcc ordering of the metal is typical when the metalloid, of much smaller size than the hosting metal, mixes as an interstitial impurity since the fcc struture has enough space in the center of the cube to included it. For instance, carbon, which is close in size and reactivity with Fe to boron, is used as a catalyzer for the growth of fcc Fe on Cu [2]. Fcc Fe has a lower magnetic moment than bcc Fe and its Curie temperature is substantially lower. In fact, it was already observed decades ago that the magnetic moment per Fe and the Curie point decreased unexpectedly in Fe-B amorphous alloys with Boron concentrations close to the eutectic point. This was actually interpreted as an indication of non-crystalline Fe having an fcc-like structure [3].

The magnetostrictive phase was never in an fcc atomic arrangement. In the case of the polycrystalline alloy, the magnetostrictive phase was bcc with the important difference with respect to pure bcc Fe that the lattice parameter was substantially enlarged: bond length increased in 0.1 A from 2.485 A to 2.58(1) A. The magnetostrictive phase of Fe in the amorphous alloys was not identified with either a bcc or an fcc structure. Fe-Fe interatomic distance was significantly enlarged to 2.63 A respect to the Fe-Fe distances in the non-magntostrictive phase. These magnetostrictive environments might be associated to the atomic environment of a related B-Fe crystal phase. Only FeB and Fe_3B crystalline phases have similar Fe-Fe distances than the found in the Fe magnetostrictive phase. FeB is less magnetic than Fe_3B, but Fe_3B is highly unstable. Its crystal structure is quite complex, similar to cementite

(Fe_3C). It has been detected in $Fe_{80}B_{20}$ amorphous alloys after annealing at relatively low temperatures (750 K) [4]. In any case, to our knowledge, the only report existing on magnetostriction in FeB and CoB system is in the amorphous alloys but not in the crystalline phases [1, 5]. FeB is in fact known because its mechanical hardness and it is used as a protecting layer in steels. However, it is very brittle and, in fact, it is considered responsible of the decrease in the magnetostriction properties of the amorphous Fe-B and Co-B alloys after annealing. Amorphous Co-B and Fe-B alloys are magnetostrictive, with magnetostrictive coefficients similar to the found in our alloys. In Fe-B, its highest magnetostrictivity is reached when the atomic boron concentration is 20% [1,5]. On the other hand, the magnetostriction in CoB is negative and it decreases with boron content [5].

The macroscopic magnetostriction coefficients were of the same order than the expected, with the exception of the magnetostriction in Co rich amorphous alloy which seemed to be higher than its experimental value [1]. However, its sign was correct. The uncertainty in the value of the magnetostriction coefficients depended mostly on the uncertainty of the coordination number deduced from the fits, which was especially high in the fit of the DiffXAFS spectra, of about 20%, since it was strongly correlated with the Debye-Waller factor. It also depended on the uncertainty in the determination of the concentration of the magnetostrictive phase, which was of the same order or bigger in some cases.

The macroscopic values deduced in the Fe rich alloys were calculated assuming that there were not magnetostrictive Co environments. If they were similar to the found in the Co rich alloy, the macroscopy magnetostrictive coefficients should be lower, since its contribution was negative.

At this point, it must be mentioned that coordination numbers obtained from the fits were smaller than what it should be if fcc arrangement was the only considered. For instance, the coordination for the non magnetostrictive phase in $(Fe_{80}Co_{20})_{20}B_{20}$ was 2.2 obtained from the fit of the EXAFS spectrum, much lower than 6.6, the value that it should have been obtained, assuming that Fe atoms arranged in an fcc-like structure, and taking into account that they should made 64% of the total number of atoms in the first shell. One possible reason to this is that there were a proportion of TM first neighbors which were strongly dispersed at too long distances due to boron intercalation contributing to the EXAFS amplitude with too little intensity. It can be seen that any of the phases in which Fe-B and Co-B can crystallize are very complex involving first TM neighbors not uniformly distributed at distances between 2.62 A and 2.92 A in FeB, 2.41 to 2.72 A in Fe_2B, and from 2.51 to 2.76 A in Fe_3B. It must be observed, however, that if there were first neighbors missing, the macroscopic magnetostriction coefficient would be even smaller than the estimated, since they would not contribute to the magnetostrictive phase. This would not affect to the magnetostriction coefficient of the phase since it depends on the ratio between the amplitudes of its spectra in DiffXAFS and EXAFS.

TM-Boron was never used in the fits. The main reason is that it has a very small cross section in the k-range of data used for the fits, and its contribution to the EXAFS spectra was therefore small [6]. An example of this is shown in figure 11, where the contribution of boron to the EXAFS spectrum was almost flat in the k-range used for the fit (from 3 A^{-1} up to 10 A^{-1}). The errors in the fits for its coordination number were large because its strong correlation with the Debye-Waller factor.

References

[1] R. C. O'Handley. Phys. Rev. B 18 (1978) 930

[2] A. Kirilyuk, J. Giergiel, J. Shen, M. Straub, and J. Kirschner. Phys. Rev. B 54 (1996) 1050

[3] J. Durand and M. Yung, *Amorphous Magnetism II*, edited by R. A. Levy and R. Hasegawa (Plenum, New York, 1977); R. Hasegawa and Ranjan Ray. J. Appl. Phys. 49(1978) 4174

[4] C. L. Chien . Phys. Rev. B 18 (1978) 1003

[5] K. Narita, J. Yamasaki, and H. Fukunaga. J. Appl. Phys. 50 (1979) 7591

[6] M. L. Fdez-Gubieda, I. Orúe, F. Plazaola, and J. M. Barandiarán. Phys. Rev. B 53 (1996) 620

[7] M. P. Ruffoni, S. Pascarelli, R. Grössinger, R. Sato Turtelli, C. Bormio-Nunes, and R. Pettifer. Phys. Rev. Lett. 101 (2008) 147202

[8] S. Pascarelli, M. P. Ruffoni, A. Trapananti, O. Mathon, G. Aquilanti, S. Ostanin, J. B. Staunton, and R. F. Pettifer. Phys. Rev. Lett. **99** (2007) 237204
[9] R.Q. Wu, L.J. Chen, A. Shick, A.J. Freeman. J. Magn. Mag. Mat. 177-181 (1998) 1216-1219

Figures

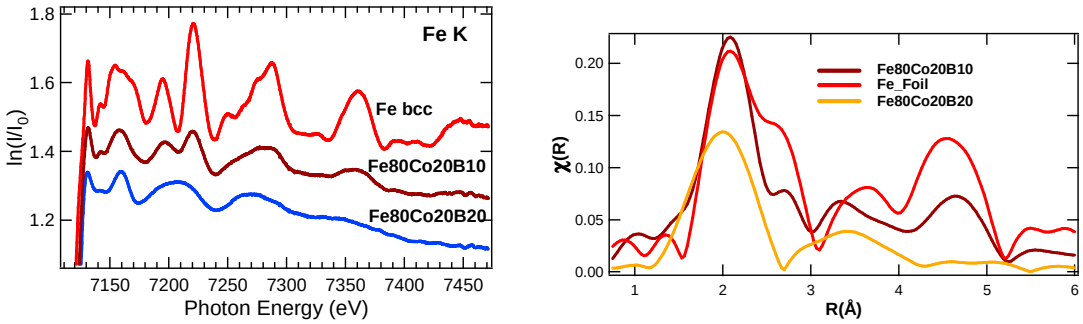

Figure 1. (a) EXAFS spectra in the Fe K edge of bcc Fe (Fe foil), $(Fe_{80}Co_{20})_{80}B_{10}$ and $(Fe_{80}Co_{20})_{80}B_{20}$; (b) Fourier transform of the χ(k) spectrum of bcc Fe, $(Fe_{80}Co_{20})_{80}B_{10}$ and $(Fe_{80}Co_{20})_{80}B_{20}$ (χ(R)). The amplitude of the Fe foil χ(R) spectrum was divided by 2.

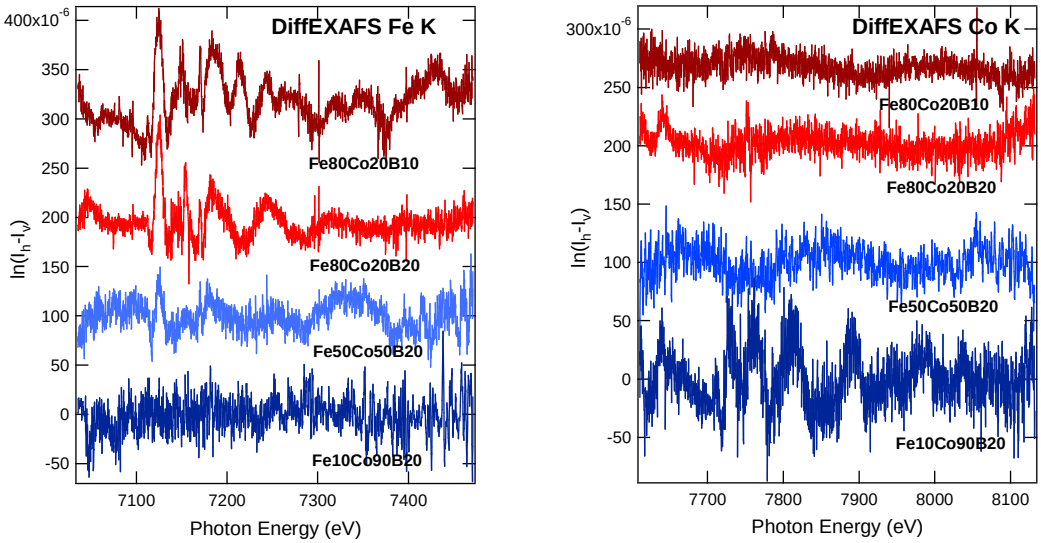

Figure 2. DiffEXAFS spectra of the FeCoB films (a) at the Fe K edge and (b) at the Co K edge.

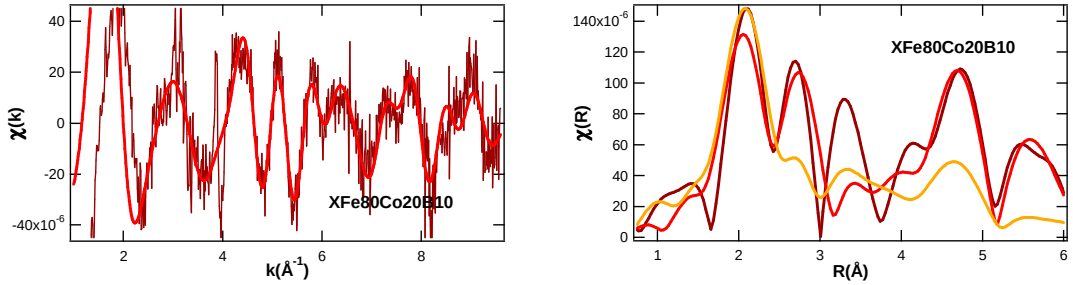

Figure 3. DiffEXAFS χ(k) and χ(R) spectrum at the Fe K edge of $(Fe_{80}Co_{20})_{80}B_{10}$ (dark red line) and its fit (red line). The yellow component in the χ(R) spectrum (right) is the EXAFS spectrum of $(Fe_{80}Co_{20})_{80}B_{10}$ inserted in the figure for comparison.

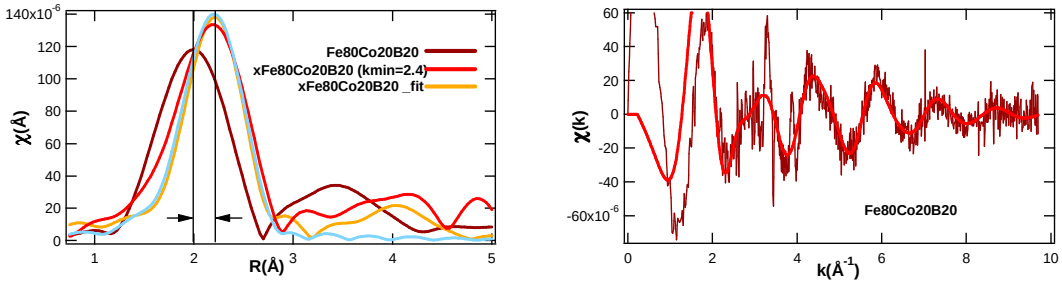

Figure 4. DiffEXAFS χ(k) and χ(R) spectrum at the Fe K edge of $(Fe_{80}Co_{20})_{80}B_{20}$ (dark red line in the χ(k) spectrum) and its fit (red line in the χ(k) spectrum). The dark red component in the χ(R) spectrum (left) is the EXAFS spectrum of $(Fe_{80}Co_{20})_{80}B_{20}$ inserted in the figure for comparison. The most intense peak at about 2 A is clearly downshifted respect to the same peak in the DiffEXAFS spectrum, demonstrating that the magnetostrictive component had a significant longer Fe-Fe distance (2.63 A) than in the EXAFS spectrum (2.45 A). The blue line is the fit of the DiffEXAFS spectrum done between 1 A and 3 A, avoiding second neighbors contributions and the high frequency noise in the spectrum. The Fe-Fe distance deduced from this fit was 2.59 A.

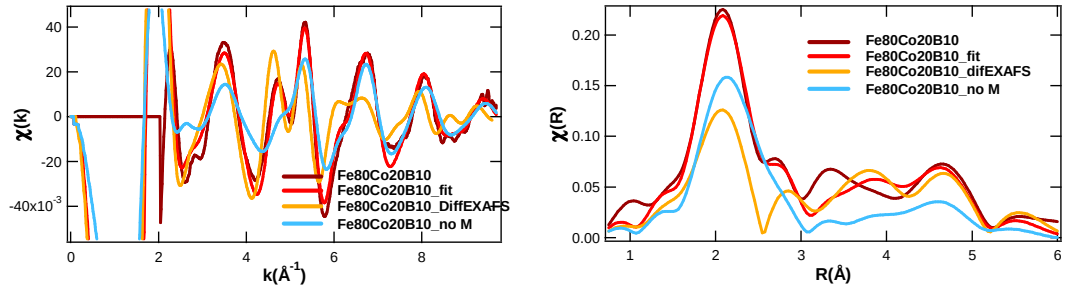

Figure 5. EXAFS spectrum of $(Fe_{80}Co_{20})_{80}B_{10}$ and its fit using two components, the one corresponding to the Fe atomic environment in the magnetostrictive phase, extracted from the DiffEXAFS, and the resulted Fe environment in the non-magnetostrictive phase.

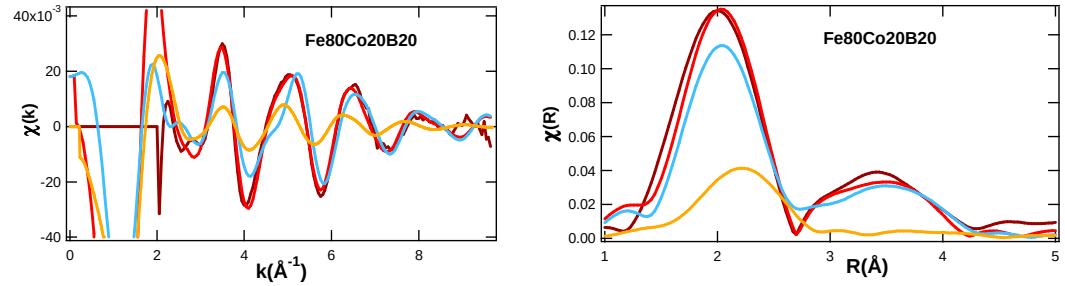

Figure 6. EXAFS spectrum of $(Fe_{80}Co_{20})_{80}B_{20}$ and its fit using two components, the one corresponding to the Fe atomic environment in the magnetostrictive phase (yellow line), extracted from the DiffEXAFS, and the resulted Fe environment in the non-magnetostrictive phase (blue line).

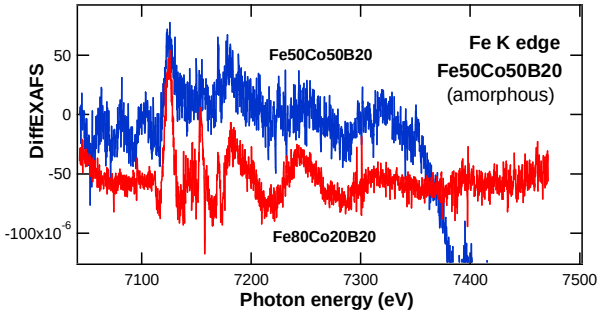

Figure 7. Comparison between the DiffEXAFS spectra of $(Fe_{80}Co_{20})_{80}B_{20}$ and $(Fe_{50}Co_{50})_{80}B_{20}$ in the Fe K edge. The spectrum of the Co rich alloy was similar to the Fe rich alloy but smaller in amplitude and much noisy.

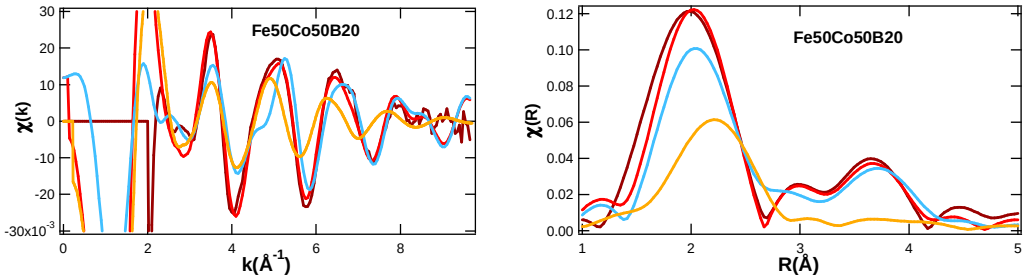

Figure 8. EXAFS spectrum of $(Fe_{50}Co_{50})_{80}B_{20}$ at the Fe K edge and its fit using two components, the one corresponding to the Fe atomic environment in the magnetostrictive phase (yellow line), extracted from the DiffEXAFS of $(Fe_{80}Co_{20})_{80}B_{20}$, and the resulted Fe environment in the non-magnetostrictive phase (blue line). As in the cose of the EXAFS spectrum of $(Fe_{80}Co_{20})_{80}B_{20}$, the intensity of the spectrum rlated to second neighbor shells is significant. The fit shows tha atoms arranged in an fcc structure, in agreement with the TM-B phase diagram obtained in bulky samples.

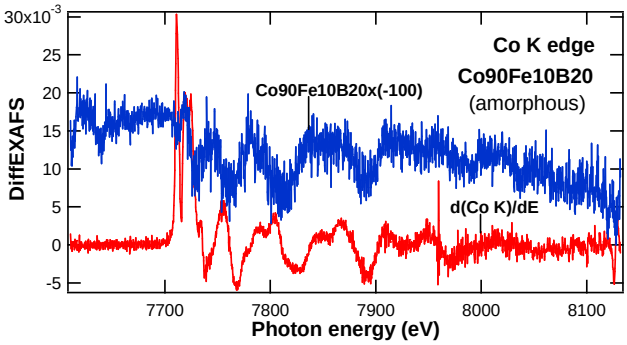

Figure 9. DiffEXAFS spectrum of $(Co_{90}Fe_{10})_{80}B_{20}$ at the Co K edge (blue line) compared with the simulated DiffEXAFS spectrum of crystalline Co (red line). The spectrum of the amorphous alloy was multiply by -100, indicating a negative strictive response to the magnetic field.

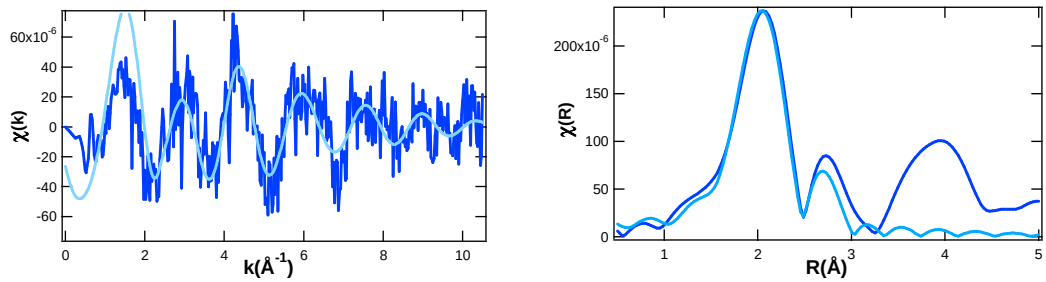

Figure 10. DiffEXAFS χ(k) and χ(R) spectrum at the Co K edge of $(Co_{90}Fe_{10})_{80}B_{20}$ (dark blue line) and its fit (light red line).

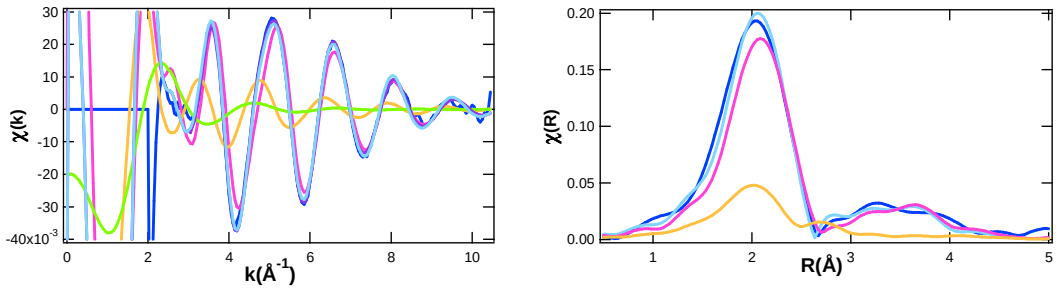

Figure 11. Fit of the EXAFS spectrum of $(Co_{90}Fe_{10})_{80}B_{20}$ at the Co K edge. The dark blue line is the spectrum, the light blue line is the fit using the magnetostrictive component extracted from DiffEXAFS (yellow line) and the non-magnetostrictive component (pink line). The green line in the figure with the χ(k) spectrum is the boron component added to the spectrum in the fit.

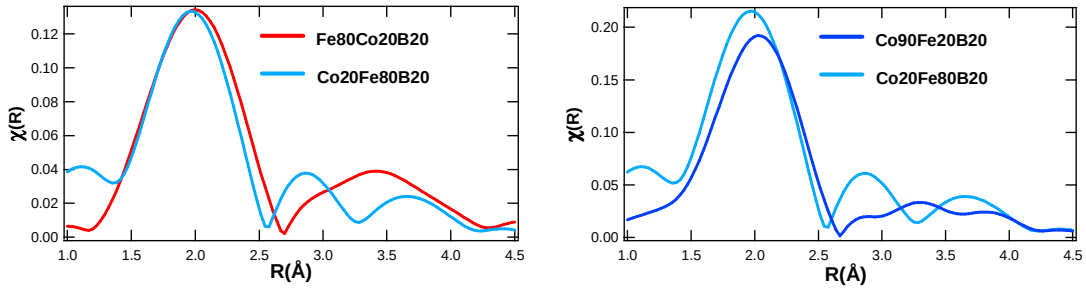

Figure 12. EXAFS spectrum (χ(R)) of $(Co_{20}Fe_{80})_{80}B_{20}$ at the Co K edge compared to the EXAFS spectra of $(Fe_{80}Co_{20})_{80}B_{20}$ at the Fe K edge and of $(Co_{90}Fe_{10})_{80}B_{20}$ at the Co K edge. It shows that the Co atomic environment is different to the Fe atomic environment in the same sample. It is also different to the Co atomic environment in the Co rich film.

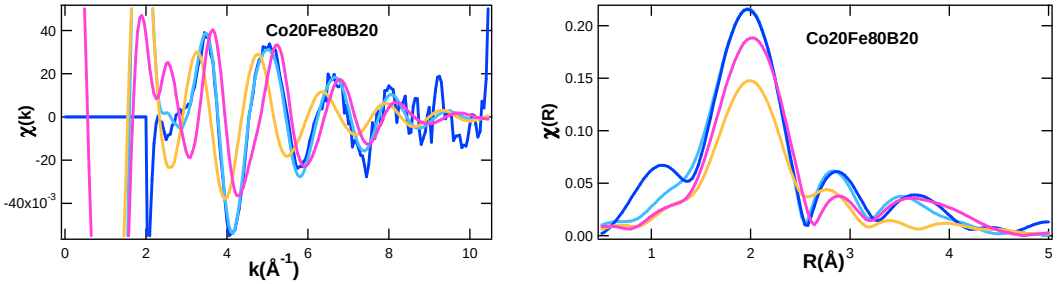

Figure 13. Fit of the EXAFS spectrum of $(Co_{20}Fe_{80})_{80}B_{20}$ at the Co K edge. The dark blue line is the spectrum, the light blue line is the fit using the magnetostrictive component extracted from DiffEXAFS (yellow line) and the non-magnetostrictive component (pink line). The magnetostrictive phase resulted to be a large proportion of the total Co atomic environments.

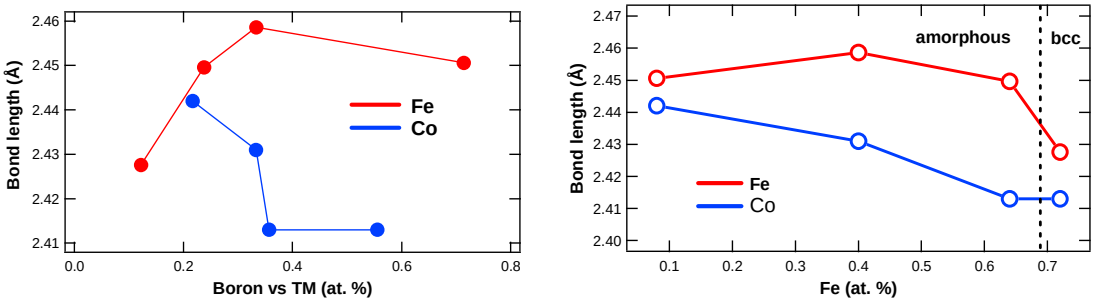

Figure 14. Left: Distance to first Transition Metal neighbor in Fe and Co versus the relative concentration of boron respect to the TM in the alloy (boron(at. %)/[boron(at. %)+TM(at. %)]. For instance, the relative concentration of boron respect to Co in $(Co_{20}Fe_{80})_{80}B_{20}$ was 20/(16+20)=0.55, and respect to Fe: 20/(20+64)=0.238). The EXAFS spectra were obtained by fluorescence in 100 nm thick films. These distances were obtained from the Fe and Co Kedge EXAFS spectra assuming one single phase model. Right: Distance to first Transition Metal neighbor in Fe and Co versus the relative concentration of Fe in the alloy.